IEEE Access
Multidisciplinary | Rapid Review | Open Access Journal

Date of publication xxxx 00, 0000, date of current version xxxx 00, 0000.

Digital Object Identifier 10.1109/ACCESS.2017.Doi Number

Voltage Compensation Method for Long-Distance Distribution Networks with Scattered Loads Based on the Cooperative Operation of DVR and Distributed Power Sources

YUKUN QIU[1], JIANYONG ZHAO[1],AND HENG NIAN[1], Senior Member, IEEE

[1]College of Electrical Engineering, Zhejiang University, Hangzhou, China

Corresponding author: Jianyong Zhao (e-mail: jyzhao@zju.edu.cn).

This work was supported by National Natural Science Foundation of China (51977194) and Experimental technology research project of Zhejiang University (SYBJS202220).

ABSTRACT The Dynamic Voltage Restorer (DVR) is an energy storage-based series compensation device that can provide voltage compensation for loads when the voltage in the power grid is out of limits. To address temporary voltage deviations in the distribution network caused by long-distance lines, fluctuating renewable energy sources, or sudden load increases, a two-layer voltage compensation model for the distribution network is established. This model combines the DVR with distributed power sources within the network. The upper layer aims to minimize the output real power of the DVR, utilizing semi-definite programming. Meanwhile, the lower layer aims to minimize network losses in the distribution network. The lower optimization model is converted into a convex form using second-order cone programming for branch flow equations and is solved by partitioning. Each partition only obtains boundary information from adjacent partitions and performs distributed solving using the alternating direction method of multipliers (ADMM). Finally, the effectiveness of this method is verified on a real distribution system in China and the IEEE 33-bus system.

INDEX TERMS Dynamic voltage restorer; ADMM; power optimization; distributed control

NOMENCLATURE

U_g	Voltage of the grid-side.
U_L	Voltage of the load-side.
I_L	Current of the DVR.
U_{DVR}	The compensation voltage of the DVR.
S_L	The complex power of the load.
P_L, Q_L	Active and reactive power of the load.
Z	The impedance of the line where the DVR is located.
R, X	Real and imaginary parts of the impedance.
U_{Lmin}, U_{Lmax}	Minimum and maximum voltage allowed for the load.
P_g, P_{loss}	The active power of the grid-side and loss on the line.
P_{DVR}, Q_{DVR}	Active and reactive power of the DVR.
V_k	Voltage of the k-th bus.
i_k	Current flowing to the k-th bus.
Z_k	The impedance of the line connecting the k-th bus to its parent bus.
r_k, x_k	Real and imaginary parts of Z_k.
S_k	The complex power of the k-th bus.
P_k, Q_k	Active and reactive power of the k-th bus.
N	Number of the bus.
p_k^L, q_k^L	Active and reactive power of the load in the k-th bus.
p_k^g, q_k^g	Active and reactive power of

	the distributed power source in the *k*-th bus.
$p_k^{g,\max}$, $q_k^{g,\max}$	The maximum active and reactive power of the distributed power source in the *k*-th bus.
ε	The permissible deviation of the voltage.
U_k	The square of the voltage magnitude at the *k*-th bus.
I_k	The square of the current magnitude at the *k*-th bus.
$\boldsymbol{X}_{\mathrm{M,C,A}}$	The state variables of the boundary between the M-th parent bus and C-th child bus in the Zone A.
$\boldsymbol{\omega}_{\mathrm{A}}$	The dual vectors constrained by the boundary equation of zone A.
ρ	Penalty parameter.
$\boldsymbol{\lambda}_{\mathrm{A}}$	Dual variable of Zone A.
t	Superscript, the number of iterations.
σ	Acceleration factor.

I. INTRODUCTION

China's remote areas are characterized by scattered loads and abundant renewable energy resources and the proportion of distributed renewable energy sources in these distribution networks is gradually increasing, which makes the problem of voltage out of limits more and more prominent [1], [2]. In order to reduce the cost of substation construction in low-load density areas, the distribution network has to extend the power supply radius and expand the coverage area under the low voltage level, leading to long distance lines with the huge line impedance voltage drop, and the end of the network is susceptible to the problem of low voltage. What's worse, the massive renewable energy access to the distribution network affects the voltage stability of the grid, and the inversely feeding is prone to occur, causing voltage to exceed the upper limits. These voltage deviations do not directly lead to high voltage ride through (HVRT) or low voltage ride through (LVRT), but there is still a risk of impacting distribution network buses. Therefore, combined with the characteristics of the long line distribution network with scattered loads, the study of voltage out of limits prevention and control program has important theoretical value and engineering significance [3].

To address voltage limit exceedances in low-load density areas, parallel-connected voltage regulation equipment is extensively deployed, including renewable energy sources such as wind turbines and photovoltaic systems, as well as reactive power compensation devices like the Static Synchronous Compensator (STATCOM). By utilizing the reactive capacity of renewable energy inverters [4] or through coordinated control of multiple parallel-connected devices [5], it is possible to compensate for line voltage drops and achieve voltage governance in distribution networks. However, the voltage control exerted by parallel-connected devices is facilitated through compensating currents. When applied to manage voltage overruns at distant buses in long-line networks with significant line impedance, this will lead to increased network losses, which can adversely affect the economic efficiency of the system's operation.

Series voltage control equipment can be operated in conjunction with parallel-connected equipment to ensure economic operation of the distribution network without exceedance voltage. This equipment include dynamic voltage restorer (DVR) and on-line tap changer (OLTC). [6] and [7] proposed cooperative control methods between OLTC and parallel-connected distributed power sources, which realizes the voltage control and guarantees the system economy.

However, the action time of OLTC in [6-7] is relatively long compared to the fully-controlled power electronic devices, and voltage compensation of the grid through OLTC still requires a long time [8], which is difficult to meet the requirements of rapid recovery from voltage overruns. DVR adopts the fully-controlled devices to control the voltage, which is more direct and rapid [9], [10], having a more prominent advantage in voltage overrun control. Combined with the large number of distributed power sources that have been constructed, the voltage problems can be managed more quickly through the cooperative operation of distributed power sources and DVRs.

Current research on DVR mainly focuses on the optimization of its converter control strategy [11], [12], [13], [14], [15], the improvement of the DVR topology in order to expand the function of DVR [16], [17], [18], and the analysis of various types of output characteristics [19], [20]. These studies focused more on the control performance of the DVR device, but did not pay attention to the impact of the DVR on the voltage and current of the rest of the distribution network, which actually changes the optimal operating point of the parallel-connected distributed power sources. Therefore, it is necessary to coordinate and optimize the control of DVR and parallel-connected equipment. However, the voltage compensation characteristics of DVR are different from OLTC. The common optimization of OLTC is realized by adding the corresponding ratio term of OLTC in the admittance matrix, but this is difficult to reflect the compensation characteristics of DVR in the same way, which shows its necessity to establish a separate optimization model for DVR compensation and optimize it in layers with the parallel-connected compensation equipment. Additionally, considering the high proportion of renewable energy in low-load density areas and its distributed form, the access of a larger number of distributed units may increase the computational pressure of double-layer coordination, and a

distributed solution algorithm can be considered to improve the adaptability of the compensation method.

Based on the above analysis, the contribution and main work of this paper can be summarized as follows:

(1) An optimization model of minimum energy output of DVR is established, and the influence of DVR output on the system is analyzed.

(2) A two-layer cooperative optimization model of distribution network voltage compensation with DVR and parallel-connected distributed power sources is established to avoid voltage being out of limits.

(3) The centralized solving methods for two-layer model based on semipositive definite programming and second-order conic programming are proposed, and alternating direction method of multipliers (ADMM) [21] with Nesterov's acceleration method is used for distributed solving.

The remainder of this paper is organized as follows. Section II presents the modeling of two-lay optimization model of distribution network voltage compensation. In Section III, the distributed solution by ADMM for the lower optimization model is given. Simulation results are presented in Section IV. Section V concludes the paper.

II. TWO-LAYER VOLTAGE COMPENSATION MODEL

The optimization model is divided into two layers according to the series and parallel-connected type, the upper layer is the DVR optimization layer and the lower layer is the distributed power sources optimization layer. The upper layer transfers the voltage information and load change information of the bus where the DVR is located to the lower layer, which updates the bus load information of the lower layer for optimization. And the lower layer will feedback the voltage result of the bus where the DVR is located to the upper layer to judge whether the voltage after the DVR compensation meets the requirements, so as to realize the effect of two-layer cooperative optimization.

A. DVR COMPENSATION CHARACTERIZATION

The voltage compensation of DVR is analyzed, ignoring the effect of harmonic voltages, the DVR can be considered as an equivalent voltage source in control, and its circuit topology when connected to the grid is shown in Figure 1. U_L and U_g are the voltage of load-side and grid-side, respectively. S_L and I_L represent the load power and current, respectively. Z is line impedance.

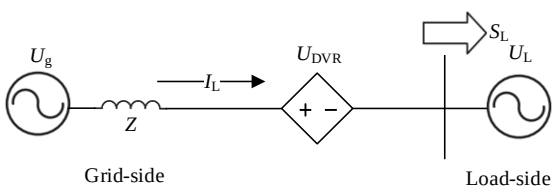

FIGURE 1. Voltage compensation model of DVR.

For distribution networks, it is necessary to ensure that the voltage of load-side bus does not exceed the limits. However, when there is a sudden change in large loads or fluctuations in renewable energy sources such as wind power and photovoltaics, the voltage will fluctuate and may exceed the limits. At this time, DVR is required to compensate for the voltage, bringing the voltage of load-side back to the allowable range, the phasor diagram of which is shown in in Figure 2. U_{Lmin} and U_{Lmax} are the minimum and maximum voltages permissible voltage for the load, respectively; φ is the power factor angle of the load; U_{DVR} is the compensating voltage phasor of DVR.

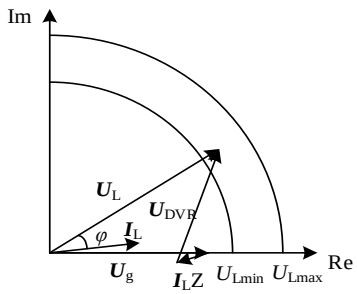

FIGURE 2. Phasor diagram of DVR voltage compensation.

The compensation of the load-side voltage by DVR changes the original line current, which can be reflected in the form of bus load information as:

$$S_L^{'} = U_g I_L^{*} = (P_L + |I_L|^2 R - P_{DVR}) + j(Q_L + |I_L|^2 X - Q_{DVR}) \quad (1)$$

where $S_L^{'}$ is the complex power of this bus after voltage compensation of DVR. P_{DVR} and P_L represent the active power consumed by the DVR and the active load of the load-side, respectively. Q_{DVR} and Q_L are the reactive power consumed by the DVR and the reactive load of the load-side, respectively. R and X are the resistance and reactance of the line.

Taking the branch system shown in Figure 1 as an example, the base voltage and power are set as 12.66 kV and 1 MW. Other simulation parameter is shown in Table I.

TABLE I
BRANCH SIMULATION PARAMETERS

U_g/p.u.	Z/p.u.	S_L/p.u.
0.900	0.0019+j0.0020	0.9+j0.7

In this branch system, the power flow from the grid-side to the load-side is 0.9+j0.7 MVA with a power factor of 0.789; the load-side voltage is raised to 1.0 p.u. by the DVR, whose output is shown in Table II.

TABLE II
OUTPUT OF DVR IN THE BRANCH

U_{DVR}/p.u.	I_L/p.u.	S_{DVR}/p.u.
0.0898+j0.1665	0.3845+j0.4186	0.2084+j0.0529

Following the voltage compensation by the DVR, the load-side voltage is restored to a nominal value of 1.0 p.u. Meanwhile, the power flow from the grid-side to the load-side is adjusted to 0.692+j0.756 MVA with the power factor changed to 0.675. This demonstrates that the DVR's voltage compensation for the load results in a substantial alteration in the power demand from the grid-side. If other distributed power sources within the distribution network fail to adjust

their output in response and persist in operating according to the initial directives, the unchanged current may intensify voltage and network loss issues on long transmission lines, which could result in considerable economic losses.

B. OPTIMIZATION MODEL OF DVR

The DVR compensation above only targets achieving a compensated voltage of 1.0 p.u. and does not take into account the optimization of the DVR output with the actual voltage safety range. As the DVR uses an energy unit (usually battery) as an energy source, it should be provided with the smallest possible active power compensation when providing voltage support, which can be regard as the objective function:

$$\min P_{\mathrm{DVR}} = P_{\mathrm{L}} - P_g + P_{\mathrm{loss}} \tag{2}$$

where P_g, P_{loss} are the active power output from the gird-side and the active power loss on the line, respectively.

Taking the grid-side voltage phasor as a reference, (2) can be further expressed in terms of line current as:

$$P_{\mathrm{DVR}} = P_{\mathrm{L}} - \mathrm{Re}(I_{\mathrm{L}}) \times U_g + \{\mathrm{Re}(I_{\mathrm{L}})^2 + \mathrm{Im}(I_{\mathrm{L}})^2\} R \tag{3}$$

At the same time, in order to keep the compensated load-side voltage within safe limits, the load current needs to satisfy the following constraints

$$U_{\mathrm{L\,min}} < \left| \frac{S_{\mathrm{L}}}{I_{\mathrm{L}}} \right| < U_{\mathrm{L\,max}} \tag{4}$$

As the low-load density areas have both voltage upper exceedance due to reverse flow and voltage lower exceedance due to increasing multiple types of loads such as electric vehicles, it makes (4) a non-convex constraint. Therefore, a quadratic constrained quadratic programming (QCQP) problem with non-convex nature is obtained from (1)-(4) as follows:

$$\begin{aligned} &\min_{x \in \mathbb{R}^2} \quad x^T A_0 x + b_0^T x \\ &\text{s.t.} \quad x^T A_i x + c_i \le 0 \quad i=1,2 \end{aligned} \tag{5}$$

where A_0 is a real symmetric positive definite matrix and one of A_1 and A_2 is a negative definite matrix.

For (5), if the heuristic algorithm is used, it may fall into the local solution to affect the optimization effect, so the semi-positive definite programming (SDP) relaxation [22] is used to convexify (5). (5) is equivalent to:

$$\begin{aligned} &\min_{x \in \mathbb{R}^2} \quad trace\left(\begin{pmatrix} 0 & 0.5b_0^{\mathrm{T}} \\ 0.5b_0 & A_0^{\mathrm{T}} \end{pmatrix} xx^{\mathrm{T}} \right) \\ &\text{s.t.} \quad trace\left(\begin{pmatrix} c_i^{\mathrm{T}} & 0.5b_0^{\mathrm{T}} \\ 0.5b_0 & A_i^{\mathrm{T}} \end{pmatrix} xx^{\mathrm{T}} \right) \le 0, (i=1,2) \\ &\qquad xx^{\mathrm{T}} \succeq 0, \qquad (xx^{\mathrm{T}})_{11} = 1 \end{aligned} \tag{6}$$

By disregarding the rank condition in (6), it serves as a solvable convex formulation. Consequently, this approach yields the optimized solution to the nonconvex QCQP problem (5), determining the active and reactive currents at the DVR's optimal output. Thereby, the output voltage of the DVR and the corresponding output power, can be derived.

The optimization of the DVR layer allows updating the external load information of the DVR installation bus for the optimal control of distributed power sources as follows.

C. OPTIMIZATION MODEL OF DISTRIBUTED POWER SOURCES

Considering a radial distribution network, which is common in low-load density areas, the voltage of buses can be regulated by distributed power sources through optimal control. In order to distinguish the direction of the line power flow, the radial distribution network is represented as a tree-like directed graph with the direction pointing from the root bus to the end bus. It is specified that the direction of the lines starts from the parent bus to the child bus, with the child bus's number always being greater than the parent bus's number. Each child bus has only one parent bus, as shown in Figure 3.

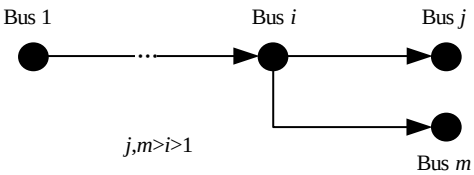

FIGURE 3. Directed tree graph of radial distribution network.

1) OBJECTIVE FUNCTION

For the optimal control of the distribution network, the economy of the system operation is considered, thus the network active power loss of the system is used as the objective function. Since each child bus has only one parent bus, the network loss of the radial network is written as

$$P_{\mathrm{loss}} = \sum_{j=N}^{1} i_j^2 r_j \tag{7}$$

where i_j and r_j are the current and resistance of the line connecting the child bus j to its parent bus. N is the number of total bus.

2) CONSTRAINTS

The constraints of a radial distribution network include the power flow constraints and the upper and lower limits of state variables. By considering the power flow variables through the child bus and marking the variables, as shown in Figure 4.

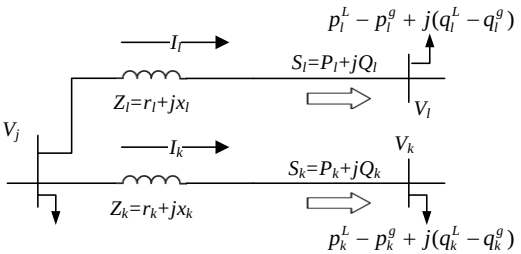

FIGURE 4. Radial distribution network flow with marked variables.

Then the equational constraints for the branch flow equation in the form of a child bus are shown below:

$$\begin{aligned} &V_j - V_k = Z_k i_k, \forall (j,k) \in N \\ &P_k + jQ_k = V_k i_k^*, \forall k \in N \\ &\sum_{k:j\to k} (P_k + r_k i_k^2) + p_j^{\mathrm{L}} - p_j^g = P_j, \forall j \in N \\ &\sum_{k:j\to k} (Q_k + x_k i_k^2) + q_j^{\mathrm{L}} - q_j^g = Q_j, \forall j \in N \\ &V_1 = V_{\mathrm{set}} \end{aligned} \tag{8}$$

where V_j is the voltage of the j-th bus; i_k and Z_k are the current flowing and impedance on the line between parent bus j and child k, respectively. $k{:}j\to k$ denotes all the child buses with j as parent bus. P_k and Q_k denote the active and reactive power flowing into bus k. p and q are the active and reactive power, respectively. The superscript 'L' denotes power from load losses and 'g' denotes power from distributed power sources. V_1 is the voltage of the root bus; V_{set} is the setting value of the voltage of root bus.

The upper and lower limits of state variables include voltage constraints, distributed power sources output constraints, as:

$$\begin{aligned} &1-\varepsilon < V_j < 1+\varepsilon \\ &p_j^g < p_j^{g,\max} \qquad \forall j \in N \\ &\left|q_j^g\right| < q_j^{g,\max} \end{aligned} \tag{9}$$

where ε is the permissible deviation of the voltage, which is 0.05 p.u. in this paper caring about farm motor in low-load density areas.

3) CONVEXIFICATION OF OPTIMAL MODELS

The distributed power sources optimal model can be expressed as (10), in which the equation constraints contain non-convex terms, which makes the global convergence of model optimization cannot be guaranteed, and it is difficult to solve the global optimal solution. Therefore, a convex relaxation is needed. Relaxation based on second-order cone program (SOCP) is used to convexify the radial distribution systems due to its tight bounder when there is no upper or lower bound on the load [23].

$$\begin{aligned} &\min_{q^g, p^g} \sum_{j=N}^{1} i_j^2 r_j \\ &\text{s.t.} \quad (8) \text{ and } (9) \end{aligned} \tag{10}$$

By eliminating the phase angles of the currents and voltages and converting the power equation constraints into the form of SOCP, (10) can be convexified as

$$\begin{aligned} &\min_{q^g, p^g} \sum_{j=N}^{1} I_j r_j \\ &s.t. \ \ U_k = U_j - 2(r_k P_k + x_k Q_k) - (r_k^2 + x_k^2) I_k, \forall (j,k) \in N \\ &\left\| \begin{matrix} 2P_k \\ 2Q_k \\ I_k - U_k \end{matrix} \right\|_2 \le I_k + U_k, \forall k \in N \\ &\sum_{k:j\to k} (P_k + r_k I_k) + p_j^{\mathrm{L}} - p_j^g = P_j, \forall j \in N \\ &\sum_{k:j\to k} (Q_k + x_k I_k) + q_j^{\mathrm{L}} - q_j^g = Q_j, \forall j \in N \\ &U_1 = V_{\mathrm{set}}^2 \\ &(1-\varepsilon)^2 < U_j < (1+\varepsilon)^2, \forall j \in N \\ &p_j^g < p_j^{g,\max}, \forall j \in N \\ &\left|q_j^g\right| < q_j^{g,\max}, \forall j \in N \end{aligned} \tag{11}$$

where U and I are the square of the voltage and current. All terms are numbered through the child buses. Through (10), the original optimization is transformed into a convex problem, which can be solved by a commercial solver and guarantees that the local optimal solution is equal to the global optimal solution. This provides a basic approach for centralized solutions.

D. TWO-LAYER COOPERATIVE COMPENSATION OPTIMIZATION PROCESS

Based on the load information provided by (1) and the voltage information obtained by (11), the voltage compensation of the DVR and the compensation capability of the distributed power sources can be interconnected through the distribution network flow to realize the cooperative compensation in case of voltage dips in the distribution network.

During the cooperative process, the optimized control of distributed power sources updates the voltage of bus where the DVR is located, which is the voltage variable 'U_g' in (3). This leads to the change of the compensation voltage of DVR, which makes a difference in the load information of the DVR located buses, i.e., 'q^{L}' and 'p^{L}' in the (11), resulting in a different 'U_g'. The iterative optimization between the DVR layer and the distributed power sources layer continues until the voltage deviation controlled by the final two-layer control satisfies the specified condition. The optimization process flowchart is shown in Figure 5. The voltage turnover is in the form of average values, i.e.:

$$U_g^{k+1} = (U_g^k + U_P^k)/2 \tag{12}$$

where superscripts denote the number of iterations and U_P is the bus voltage of DVR installation location calculated from distributed power sources layer.

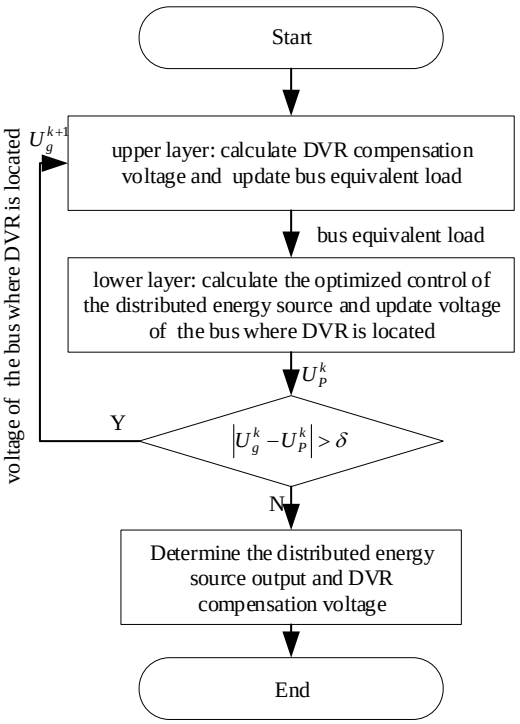

FIGURE 5. -Two-layer optimization process.

III. DISTRIBUTED OPTIMIZATION SOLUTION BASED ON ADMM

(11) represents a centralized algorithm with a specific requirement on the central processor and global communication. In order to reduce the pressure of global communication, a distributed optimization approach is proposed for solving (11), which divides the distribution network into multiple zones controlled by different sub-controllers. The sub-controller does not need to consider distributed power sources outside its own zone, which strengthens the adaptability to distributed power sources access.

A. CENTRALIZED MODEL DECOMPOSITION

Radial distribution networks can be partitioned that is based on geographic location or through clustering algorithms [24], which contain one or more buses in each zone, as shown in Figure 6. The buses within Zone-I are denoted by {1,2,3,4,5}, while Zone-II encompasses the buses {6,7,8,9,10,11}. Zone-III consists of the buses {12,13,14,15,16,17}. The boundary buses that delineate the interface between Zone-I and Zone-II are identified by {5,6}, and those that mark the boundary between Zone-I and Zone-III are represented by {5,12}. These boundary buses are interconnected through a boundary connected branch. The state variables of the boundary connected branch include the voltage of the parent bus and the child bus, as well as the active and reactive power of child bus, i.e., $\boldsymbol{X}_{\mathrm{M,C},i}=\{U_{\mathrm{M}}, U_{\mathrm{C}}, P_{\mathrm{C}}, Q_{\mathrm{C}}\}$, where M is the number of the parent bus at the boundary, C is the number of the child bus at the boundary, and i is the zone number.

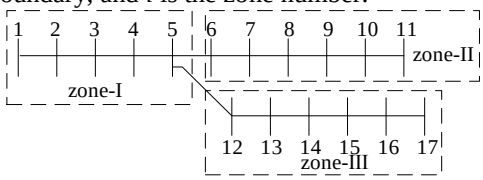

FIGURE 6. Zone division of radial distribution network.

The state variables of the boundary branches need to be added to the constraints when the centralized optimization problem has been decomposed to ensure that the final result matches the original optimization result. The optimization model of distributed power sources based on the distribution networks partition is shown in (13).

$$\begin{aligned} &\min \sum_{i=1}^{W} f_i(\boldsymbol{x}_i) \\ &\text{s.t. } h_i(\boldsymbol{x}_i)=0, i\in W \\ &\quad g_i(\boldsymbol{x}_i)\le 0, i\in W \\ &\quad \boldsymbol{X}_{\mathrm{M,C},i}=\boldsymbol{X}_{\mathrm{M,C},j}, i,j\in W \end{aligned} \tag{13}$$

where $f_i(\boldsymbol{x}_i)$ is the objective function of the subproblem in zone-i. W is the number of zones. $h_i(\boldsymbol{x}_i)$ and $g_i(\boldsymbol{x}_i)$ are the equation constraints and inequality constraints of the subproblems, respectively. $\boldsymbol{x}_i$ denotes all the state variables in zone-i, including the power and voltage of each bus, the line currents in the zone, and the output of the distributed power source. Zone-j denotes the adjacent zone connected to zone-i through a boundary branch. $\boldsymbol{X}_{\mathrm{M,C},i}$ is a part of x_i, while $\boldsymbol{X}_{\mathrm{M,C},j}$ is a boundary branch variable of another zone j. Only if the state variables of the boundary branches of two adjacent zones are all in the same, the distributed solution can be guaranteed to be consistent with the centralized one. These variables are consensus variables that ensure the solutions from different zones are consistent.

The equation constraints, inequality constraints of the subproblem in (13) may be specifically represented as shown in equation (14).

$$\begin{aligned} &U_k = U_j - 2(r_k P_k + x_k Q_k) - (r_k^2 + x_k^2) I_k \\ &\left\| \begin{matrix} 2P_j \\ 2Q_j \\ I_j - U_j \end{matrix} \right\|_2 \le I_j + U_j \\ &\sum_{k:j\to k} (P_k + r_k I_k) + p_j^L - p_j^g = P_j \\ &\sum_{k:j\to k} (Q_k + x_k I_k) + q_j^L - q_j^g = Q_j \\ &U_1 = V_{\mathrm{set}}^2 \\ &(1-\varepsilon)^2 < U_j < (1+\varepsilon)^2 \\ &p_j^g < p_j^{g,\max} \\ &\left| q_j^g \right| < q_j^{g,\max} \end{aligned} \tag{14}$$

where bus k is the child bus of j. When the bus j is a boundary bus of the zone (means bus k is not in this zone), the zone where the bus j is located estimates and corrects the voltage and power of the bus k through (13), as shown in Figure 7.

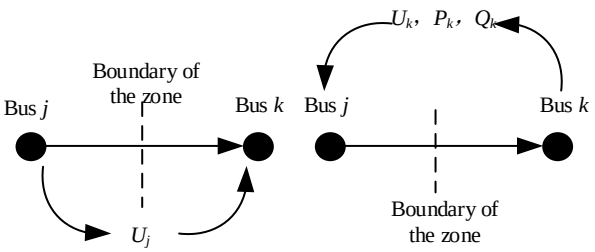

FIGURE 7. Transfer method of zone state variables.

B. DISTRIBUTED SOLVING

The subproblems can be solved in a distributed way by ADMM. The distributed optimization when the radial distribution network is decomposed into two zones A and B is used as an example for the distributed solution based on ADMM.

The subproblems of the optimization problem are established in A and B, assuming that the boundary buses of the two zones are bus M and bus C, respectively. The corresponding augmented Lagrange function can be established as:

$$\begin{aligned} L_A(\boldsymbol{x}_A, \boldsymbol{X}_{\mathrm{M,C},B}, \boldsymbol{\omega}_A) &= f_A(\boldsymbol{x}_A) + \boldsymbol{\omega}_A^T(\boldsymbol{X}_{\mathrm{M,C},A} - \boldsymbol{X}_{\mathrm{M,C},B}) \\ &\quad + \frac{\rho}{2}\left\|\boldsymbol{X}_{\mathrm{M,C},A} - \boldsymbol{X}_{\mathrm{M,C},B}\right\|_2^2 \\ L_B(\boldsymbol{x}_B, \boldsymbol{X}_{\mathrm{M,C},A}, \boldsymbol{\omega}_B) &= f_B(\boldsymbol{x}_B) + \boldsymbol{\omega}_B^T(\boldsymbol{X}_{\mathrm{M,C},B} - \boldsymbol{X}_{\mathrm{M,C},A}) \\ &\quad + \frac{\rho}{2}\left\|\boldsymbol{X}_{\mathrm{M,C},B} - \boldsymbol{X}_{\mathrm{M,C},A}\right\|_2^2 \end{aligned} \tag{15}$$

where $\boldsymbol{\omega}_\mathrm{A}$ and $\boldsymbol{\omega}_\mathrm{B}$ are the dual vectors constrained by the boundary equation of zone A and B, respectively. ρ is the penalty parameter.

Set $\boldsymbol{\lambda}=\boldsymbol{\omega}/\rho$, which combines the dual parameter and penalty parameter in (15):

$$\begin{aligned} L_A &= f_A(\boldsymbol{x}_A) + \frac{\rho}{2}\left\|\boldsymbol{X}_{\mathrm{M,C},A} - \boldsymbol{X}_{\mathrm{M,C},B} + \boldsymbol{\lambda}_A\right\|_2^2 - \frac{\rho}{2}\left\|\boldsymbol{\lambda}_A\right\|_2^2 \\ L_B &= f_B(\boldsymbol{x}_B) + \frac{\rho}{2}\left\|\boldsymbol{X}_{\mathrm{M,C},B} - \boldsymbol{X}_{\mathrm{M,C},A} + \boldsymbol{\lambda}_B\right\|_2^2 - \frac{\rho}{2}\left\|\boldsymbol{\lambda}_B\right\|_2^2 \end{aligned} \tag{16}$$

State variables are updated by:

$$\begin{aligned} \boldsymbol{x}_A^{t+1} &= \arg\min\ f_A(\boldsymbol{x}_A) + \frac{\rho}{2}\left\|\boldsymbol{X}_{\mathrm{M,C},A}^t - \boldsymbol{X}_B^t + \boldsymbol{\lambda}_A^t\right\|_2^2 \\ \boldsymbol{x}_B^{t+1} &= \arg\min\ f_B(\boldsymbol{x}_B) + \frac{\rho}{2}\left\|\boldsymbol{X}_{\mathrm{M,C},B}^t - \boldsymbol{X}_A^t + \boldsymbol{\lambda}_B^t\right\|_2^2 \\ \boldsymbol{X}_B^{t+1} &= X_{\mathrm{M,C},B}^{t+1} \\ \boldsymbol{X}_A^{t+1} &= X_{\mathrm{M,C},A}^{t+1} \end{aligned} \tag{17}$$

where t is the number of iterations.

Dual variables are updated by:

$$\begin{aligned} \boldsymbol{\lambda}_A^{t+1} &= \boldsymbol{\lambda}_A^t + \boldsymbol{X}_{\mathrm{M,C},A}^{t+1} - \boldsymbol{X}_B^{t+1} \\ \boldsymbol{\lambda}_B^{t+1} &= \boldsymbol{\lambda}_B^t + \boldsymbol{X}_{\mathrm{M,C},B}^{t+1} - \boldsymbol{X}_A^{t+1} \end{aligned} \tag{18}$$

As a result, iterative solutions for the subproblems can be independently pursued within each zone. With the solution, each zone is able to optimize and control the distributed power sources within its domain. This strategy reduces the need for data transfer and increases computation speeds

The results of the distributed computation are transmitted to the controller of the DVR. When the voltage of bus cannot be supported by the distributed power source, the DVR will calculate the compensation voltage according to (1) and updates the load information in which DVR is located according to (3), performing the next round of the distributed computation.

C. ACCELERATED SOLVING OF ADMM

ADMM has a convergence rate of O(1/k), which converges to a solution near a medium accuracy after a certain number of runs [25], and a large number of iterations are required to further improve the accuracy. The Nesterov's method [26] is used to accelerate the speed of convergence, which is applicable to the first-order problems, is used to accelerate the ADMM to increase the convergence rate to O(1/k^2):

$$\begin{aligned} \sigma_0 &= 1 \\ \sigma_{t+1} &= \frac{1+\sqrt{1+4\sigma_t^2}}{2} \end{aligned} \tag{19}$$

where σ is the acceleration factor whose value iterates itself as the iteration proceeds while t is the number of iterations. At that time, the dual variables are updated in a new way:

$$\begin{aligned} \boldsymbol{\lambda}_A^{t+1} &= \boldsymbol{\lambda}_A^t + \frac{\sigma_{t-1}-1}{\sigma_t}(\boldsymbol{\lambda}_A^t - \boldsymbol{\lambda}_A^{t-1}) \\ \boldsymbol{\lambda}_B^{t+1} &= \boldsymbol{\lambda}_B^t + \frac{\sigma_{t-1}-1}{\sigma_t}(\boldsymbol{\lambda}_B^t - \boldsymbol{\lambda}_B^{t-1}) \end{aligned} \tag{20}$$

The convergence speed of ADMM can be improved after updating the dual variables by (20).

IV. CASE STUDY

A. PARAMETERIZATION OF THE CASE

A practical three-phase balanced 233km, 10.5 kV radial feeder with high penetration of distributed PV units located in Guoluo, Qinghai Province, China, is selected to verify the effectiveness of the proposed method, which exhibits high penetration of distributed power sources (detailed parameters are shown in the APPENDIX A). This distribution network is characterized by a substantial power supply radius, significant voltage drops, and the potential to breach the lower voltage limit. Concurrently, the integration of stochastic and volatile distributed power source introduces the risk of surpassing the upper voltage limit.

The distribution network structure is shown in Figure 8, which is divided into three zones. Buses 5, 6, 9 and 15 are equipped with controllable active power sources such as gas turbine and energy storage with a maximum output power of 0.500 MW. Buses 1, 8, 11 and 14 are equipped with 0.4 MVAr static var compensators (SVCs). Bus 18 is equipped with a PV with a maximum power of 0.15 MW, which is not controllable. DVR is accessed at bus 17. The upper and lower voltage limits are set as 0.95 p.u. to 1.05 p.u., and the iterative number is 100.

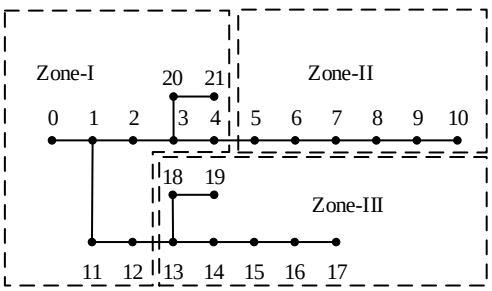

FIGURE 8. Distribution system at a location in Guoluo, Qinghai Province, China.

B. RESULT OF THE CASE

Voltage regulation of the distribution network is carried out at the moment when the PV output is 60% of the maximum value. The network active power loss is 100.05 kW and there are several voltages breach the upper limit or the lower limit. After the two-layer optimization, the network active power loss is reduced to 78.75 kW, all the voltages are restored to 0.95-1.05 p.u., as shown in Figure 9. Bus 9 and bus 10, which have the largest voltage deviation, are under the control of the proposed method and achieve a compensated recovery of the voltage across the upper limit, and for the low-voltage in bus 17, it also recovers to 0.95 p.u. The two-layer optimization proposed in this paper can effectively reduce the network active power loss and can regulate the voltage within the safe range to maintain the normal voltage of the bus by DVR when the voltages exceed the limit.

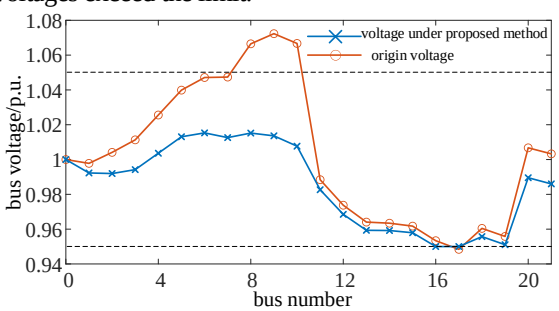

FIGURE 9. Comparison of voltage of distribution system in Guoluo before and after optimization.

The active and reactive power iteration curves of each distributed power source are shown in Figure 10 and Figure 11, respectively. Convergence can be achieved in fewer iterations, which can lessen the burden of inter-regional communication and speed up the process of the voltage overrun problem.

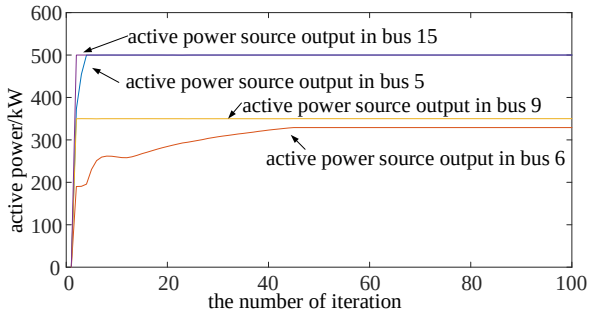

FIGURE 10. Iteration Curves of active power source output.

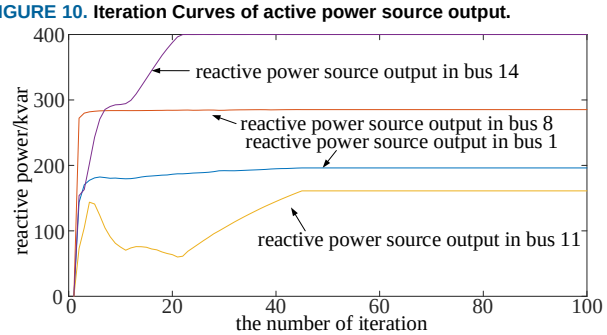

FIGURE 11. Iteration Curves of reactive power source output.

C. ALGORITHM PERFORMANCE COMPARISON

To verify the performance of the proposed method, the results for DVR-only and distributed power sources-only (which is the most common method of voltage compensation) scenarios are compared, as shown in Table III. When voltage compensation is provided solely by the DVR, the network active power loss in the system increases, and the voltage overrun cannot be completely managed. Conversely, when voltage compensation is provided solely by distributed power sources which is a conventional voltage compensation method, some buses still exceed the lower voltage limit. Only through the two-layer synergistic compensation proposed in this paper, the voltage overruns can be eliminated and the network active power loss can be reduced.

TABLE III
COMPARISON BETWEEN DVR, DISTRIBUTION POWER SOURCES AND TWO-LEVEL OPTIMIZATION

Result	Proposed Method	DVR Only	Distributed Power Sources Only
Network Active Power loss/kW	78.75	104.48	82.23
Voltage of Bus	all within the safety range.	some exceed the lower limit, and some exceed the upper limit	some exceed the lower limit

In addition, the effectiveness of the proposed method is compared with that of the centralized optimization method. The centralized method uses 1) primal dual interior point method and 2) SOCP. The primal dual interior point method

directly solves (9), while the SOCP solves the centralized model (10) The distributed power sources outputs calculated by the two-layer optimization method and the two centralized methods are shown in Table IV. It can be seen that the output power under the two-layer optimization control is the same as the output under the centralized optimization control using SOCP, and it is similar to the result by the primal dual interior point method. Compared to the two centralized algorithms, the two-layer optimization proposed in this paper does not require centralized controllers, and each controller involves a smaller number of zone's buses, which reduces the computational burden on the zone controllers.

TABLE IV
OUTPUT OF DISTRIBUTION POWER SOURCES

Source Type	Location	Centralized Method 1)	Centralized Method 2)	Proposed Method
Active Power Source/kW	5	500.00	499.99	499.99
	6	330.63	329.66	329.66
	9	350.00	350.04	350.04
	15	500.00	500.00	500.00
Reactive Power Source/kvar	1	196.37	196.37	196.37
	8	285.30	285.27	285.27
	11	162.60	162.61	162.61
	14	400.00	399.99	399.99

D. ALGORITHM ADAPTATION VALIDATION

In order to verify the adaptability of proposed method, the IEEE 33-bus system is used for the validation. The zones of the IEEE 33-bus system are shown in Figure 12. Buses 3, 12, 15, 16 and 25 are equipped with controllable active power sources with a maximum output power of 0.35 MW. Buses 3, 12, 16, 23, 27 and 30 are equipped with 0.35 MVAr SVCs. Buses 18, 20, 27 and 28 are equipped with a PV with a maximum power of 0.15 MW, which is not controllable. DVRs are accessed at bus 17 and 32. The load rate at bus 32 is set to 2. Consider 24 different load rates and normalized lightings which can be forecasted [27] following the variation curves as shown in Figure 13 and Figure 14. The network active power loss during 24 hours of the IEEE 33-bus system are shown in Figure 15 and the voltage at bus 32 is shown in Figure 16. According to Figure 15, At the 9 time, there is a simultaneous increase in the output power of the PV system and the load rate, which prevents the active power from being locally consumed. Consequently, it is directed to other buses, leading to an increase in line active power loss. After the 13 time, while the PV output power diminishes, the load rate continues to rise, necessitating the root bus to supply more active power. This additional active power further exacerbates the line's active power loss, resulting in an elevated growth rate of active power loss during this period. It is not until the 14 and 15 time, when the load rate decreases more rapidly than the reduction in PV system output, that the distribution network can achieve a balance with the bus loads in situ, thereby reducing the network active power loss.

The two-layer optimization method can achieve the optimal control at each moment point under different load cases and light intensity, which effectively reduces the network active power loss with an average of 20 kW and compensates voltage.

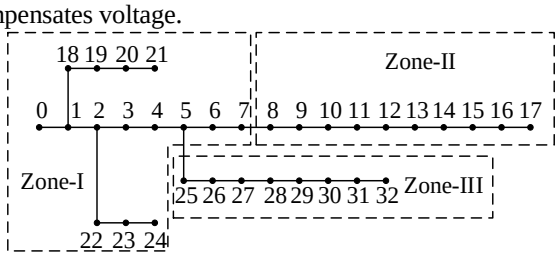

FIGURE 12. IEEE 33-bus distribution system with 3 zones.

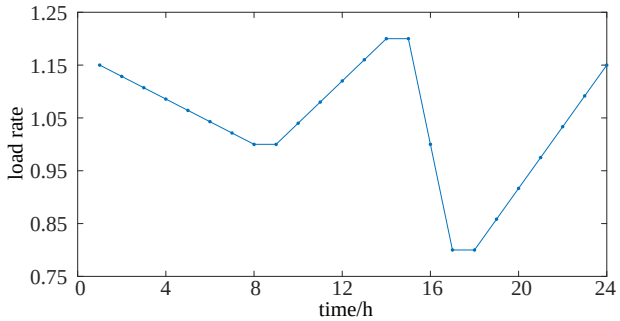

FIGURE 13. Load rate curve.

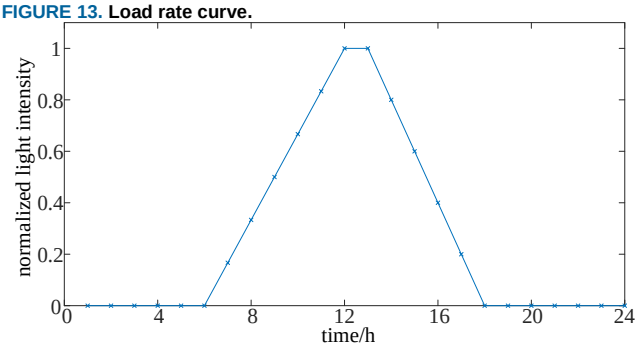

FIGURE 14. Normalized light intensity.

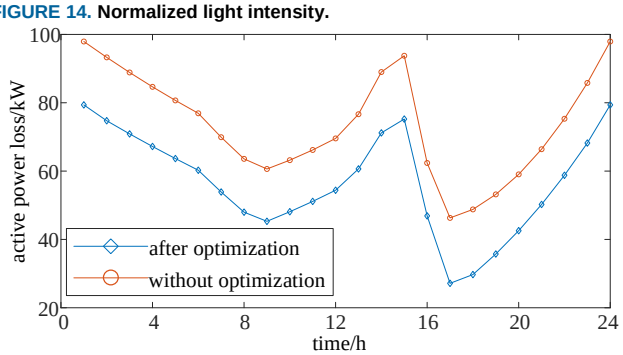

FIGURE 15. Comparison of network active power loss of IEEE 33-bus system before and after two-layer optimization.

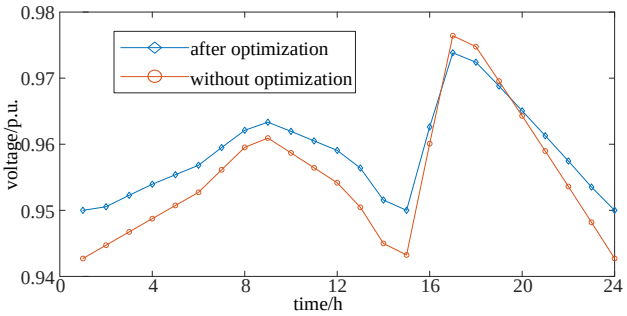

FIGURE 16. Comparison of voltage of bus 32 before and after two-layer optimization.

V. CONCLUSION

A two-layer optimization model of distribution network voltage compensation with DVR and distributed power sources and its distributed solution method are proposed in this paper. The upper layer of the model takes the minimum output active power of DVR as the objective, controls the voltage and phase of DVR compensation. The changed load information is fed back to the lower layer; while the lower layer takes the network active power loss as the objective, and controls the distributed power sources outputs in different zones of the distribution network.

In the solution of the two-layer model, there are the following features: 1) the parent bus and the child bus are divided according to the radial distribution network model; 2) ADMM is used for distributed solution to reduce the communication pressure and controller processing pressure; 3) an accelerated algorithm is used for the convergence of the ADMM algorithm, which improves the convergence speed.

Finally, the effectiveness of the proposed two-layer optimization is verified by the application of the algorithm on a real distribution network in China and IEEE 33-bus distribution system. However, harmonics and unbalance problems due to excessive penetration of power electronic equipment should be further studied.

APPENDIX A

The loads and line parameters of the distribution network in Guoluo are shown in Table AI and Table AII.

TABLE AI
LOAD OF THE DISTRIBUTION NETWORK IN GUOLUO

Bus	Active Load/kW	Reactive Load /kVAr
1	114.5	22.6
2	125.95	24.86
3	128.24	25.312
4	0	0
5	0	0
6	0	0
7	120	62
8	125	70
9	100	54
10	100	50
11	115.645	22.826
12	112.21	22.148
13	113.355	22.374
14	103.05	20.34
15	105.34	20.792
16	107.63	21.244
17	241.824	47.7312
18	121.37	23.956
19	123.66	24.408
20	116.79	23.052
21	119.08	23.504

TABLE AII
LINE PARAMETER OF THE DISTRIBUTION NETWORK IN GUOLUO

Branch	From Bus	To Bus	Resistance/Ω	Reactance/Ω
1	0	1	1.224	0.658512
2	1	2	1.9584	1.053619
3	2	3	1.4688	0.790214
4	3	4	1.4688	0.790214
5	4	5	1.4688	0.790214
6	5	6	1.4688	0.790214
7	6	7	1.4688	0.790214
8	7	8	6.56	7.22
9	8	9	5.31	5.84
10	9	10	3.22	3.54
11	1	11	1.7136	0.921917
12	11	12	2.448	1.317024
13	12	13	2.2032	1.185322
14	13	14	1.836	0.987768
15	14	15	1.4688	0.790214
16	15	16	1.7136	0.921917
17	16	17	1.4688	0.790214
18	13	18	1.4688	0.790214
19	18	19	2.6928	1.448726
20	3	20	1.4688	0.790214
21	20	21	2.2032	1.185322

REFERENCES

[1] Y. Zhao, S. Xia, J. Zhang, Y. Hu and M. Wu, "Effect of the Digital Transformation of Power System on Renewable Energy Utilization in China," *IEEE Access*, vol. 9, pp. 96201-96209, 2021.

[2] L. Zhan, B. Hu, L. Chen, Y. Liao, M. Li and H. Nian, "Transient Stability Enhancement of Current Limited-GFM Inverters Based on Varying Virtual Impedance," *IEEE Trans. Ind. Electron.*, early access, Jun. 11, 2024, doi: 10.1109/TIE.2024.3395781.

[3] N. Wight, S. Alahakoon and P. Pledger, "Voltage drop and unbalance compensation in long distance medium voltage distribution lines a feasibility study," 2015 IEEE 10th International Conference on Industrial and Information Systems (ICIIS), Peradeniya, Sri Lanka, 2015, pp. 1-6.

[4] Y. Hu, W. Liu and W. Wang, "A Two-Layer Volt-Var Control Method in Rural Distribution Networks Considering Utilization of Photovoltaic Power," *IEEE Access*, vol. 8, pp. 118417-118425, 2020.

[5] W. Rohouma, M. Metry, R. S. Balog, A. A. Peerzada, M. M. Begovic and D. Zhou, "Analysis of the Capacitor-Less D-STATCOM for Voltage Profile Improvement in Distribution Network With High PV Penetration," *IEEE Open Journal of Power Electron.*, vol. 3, pp. 255-270, 2022.
[6] W. Jiao, J. Chen, Q. Wu, C. Li, B. Zhou and S. Huang, "Distributed Coordinated Voltage Control for Distribution Networks With DG and OLTC Based on MPC and Gradient Projection," *IEEE Trans. Power Syst.*, vol. 37, no. 1, pp. 680-690, Jan. 2022.
[7] Z. Tang, D. J. Hill and T. Liu, "Distributed Coordinated Reactive Power Control for Voltage Regulation in Distribution Networks," *IEEE Trans. Smart Grid*, vol. 12, no. 1, pp. 312-323, Jan. 2021.
[8] D. Hu, Y. Peng, W. Wei, T. Xiao, T. Cai, and W. Xi, "Multi-timescale Deep Reinforcement Learning for Reactive Power Optimization of Distribution Network," *Proceedings of the Chinese Society of Electrical Engineering*, vol. 42, no. 14, pp. 5034–5044, 2022.
[9] J. Wang, Y. Xing, H. Wu and T. Yang, "A Novel Dual-DC-Port Dynamic Voltage Restorer With Reduced-Rating Integrated DC–DC Converter for Wide-Range Voltage Sag Compensation," *IEEE Trans. Power Electron.*, vol. 34, no. 8, pp. 7437-7449, Aug. 2019.
[10] J. Roldán-Pérez, A. García-Cerrada, M. Ochoa-Giménez and J. L. Zamora-Macho, "Delayed-Signal-Cancellation-Based Sag Detector for a Dynamic Voltage Restorer in Distorted Grids," *IEEE Trans. Sust. Ener.*, vol. 10, no. 4, pp. 2015-2027, Oct. 2019.
[11] C. Kumar and M. K. Mishra, "Predictive Voltage Control of Transformerless Dynamic Voltage Restorer," *IEEE Trans. Ind. Electron.*, vol. 62, no. 5, pp. 2693-2697, May 2015.
[12] A. P. Torres, P. Roncero-Sánchez and V. F. Batlle, "A Two Degrees of Freedom Resonant Control Scheme for Voltage-Sag Compensation in Dynamic Voltage Restorers," *IEEE Trans. Power Electron.*, vol. 33, no. 6, pp. 4852-4867, June 2018.
[13] S. Biricik, H. Komurcugil, N. D. Tuyen and M. Basu, "Protection of Sensitive Loads Using Sliding Mode Controlled Three-Phase DVR With Adaptive Notch Filter," *IEEE Trans. Ind. Electron*, vol. 66, no. 7, pp. 5465-5475, July 2019.
[14] D. G. A. Krishna, K. Anbalagan, K. K. Prabhakaran and S. Kumar, "An Efficient Pseudo-Derivative-Feedback-Based Voltage Controller for DVR Under Distorted Grid Conditions," *IEEE Journal of Emerging and Selected Topics in Industrial Electronics*, vol. 2, no. 1, pp. 71-81, Jan. 2021.
[15] A. Parreño Torres, P. Roncero-Sánchez, J. Vázquez, F. J. López-Alcolea and E. J. Molina-Martínez, "A Discrete-Time Control Method for Fast Transient Voltage-Sag Compensation in DVR," *IEEE Access*, vol. 7, pp. 170564-170577, 2019.
[16] P. Ghavidel, M. Farhadi, M. Dabbaghjamanesh, A. Jolfaei and M. Sabahi, "Fault Current Limiter Dynamic Voltage Restorer (FCL-DVR) With Reduced Number of Components," *IEEE Journal of Emerging and Selected Topics in Industrial Electronics*, vol. 2, no. 4, pp. 526-534, Oct. 2021.
[17] F. Jiang, S. Cheng, C. Tu, Q. Guo, Q. Li and C. Chen, "Optimum control scheme of output voltage based on cascaded H-bridge DVR," *CSEE Journal of Power and Energy Systems*, vol. 6, no. 2, pp. 249-258, June 2020.
[18] Q. Guo, C. Tu, F. Jiang, R. Zhu and J. Gao, "Improved Dual-Functional DVR With Integrated Auxiliary Capacitor for Capacity Optimization," *IEEE Trans. Ind. Electron.*, vol. 68, no. 10, pp. 9755-9766, Oct. 2021.
[19] Y.-Y. Liu, X.-N. Xiao, and Y.-H. Xu, "Characteristics analysis on energy steady compensation for dynamic voltage restorer," *Proceedings of the Chinese Society of Electrical Engineering*, vol. 30, no. 13, pp. 69–74, 2010.
[20] C. Tu, L. Zhang, Q. Guo, F. Jiang, and Y. Sun, "Study on Maximum Level Output Characteristics of Dynamic Voltage Restorer Based on HPWM Modulation," *Power System Technology*, vol. 43, no. 8, pp. 2942–2951, 2019, doi: 10.13335/j.1000-3673.pst.2018.1036.
[21] DR. H. "A Survey on Some Recent Developments of Alternating Direction Method of Multipliers," *Journal of the Operations Research Society of China*, vol. 10, pp. 1–52, Jan. 2022.
[22] L. Vandenberghe, S. Boyd, "Semidefinite Programming," *SIAM Review*, vol. 38, no. 1, pp. 49-95, March 1996.
[23] M. Farivar and S. H. Low, "Branch Flow Model: Relaxations and Convexification—Part I," *IEEE Trans. Power Syst.*, vol. 28, no. 3, pp. 2554-2564, Aug. 2013.
[24] Y. Bansal, R. Sodhi, S. Chakrabarti and A. Sharma, "A Novel Two-Stage Partitioning Based Reconfiguration Method for Active Distribution Networks," *IEEE Trans. Power Delivery*, vol. 38, no. 6, pp. 4004-4016, Dec. 2023.
[25] Stephen Boyd; Neal Parikh; Eric Chu; Borja Peleato; Jonathan Eckstein, Distributed Optimization and Statistical Learning via the Alternating Direction Method of Multipliers , now, 2011.
[26] Nesterov Y E. "A method for solving the convex programming problem with convergence rate O (1/k^ 2)," *Dokl. akad. nauk Sssr.*, vol. 269, no. 3, pp. 543-547, 1983.
[27] T. Yao et al., "Very Short-Term Forecasting of Distributed PV Power Using GSTANN," in CSEE Journal of Power and Energy Systems, vol. 10, no. 4, pp. 1491-1501, July 2024.

YUKUN QIU and all authors may include biographies. Biographies are often not included in conference-related papers. This author became a Member (M) of IEEE in 1976, a Senior Member (SM) in 1981, and a Fellow (F) in 1987. The first paragraph may contain a place and/or date of birth (list place, then date). Next, the author's educational background is listed. The degrees should be listed with type of degree in what field, which institution, city, state, and country, and year the degree was earned. The author's major field of study should be lower-cased.

JIANYONG ZHAO received the B.Eng. degree from Qingdao University of Science and Technology in 2009 and the M.Eng. degree from Anhui University of Science and Technology in 2012, both in control engineering. From 2019 to date, he has been pursuing a doctorate in electrical engineering at the College of Electrical Engineering, Zhejiang University.

His current research interests include optimal configuration of integrated energy systems and energy management technology. He has published more than 20 papers and has 12 authorized invention patents.

HENG NIAN received the B.Eng. degree and the M.Eng. degree from HeFei University of Technology, China, and the Ph.D. degree from Zhejiang University, China, in 1999, 2002, and 2005 respectively, all in electrical engineering. From 2005 to 2007, he was as a Post-Doctoral with the College of Electrical Engineering, Zhejiang University, China.

In 2007, he was promoted as an associate professor. Since 2016, he has been a Full Professor at the College of Electrical Engineering, Zhejiang University, China. From 2013 to 2014, he was a visiting scholar at the Department of Electrical, Computer, and System Engineering, Rensselaer Polytechnic Institute, Troy, NY. His current research interests include the optimal design and operation control for wind power generation system. He has published more than 40 IEEE/IET Transaction papers and holds more than 20 issued/pending patents.